


BRIEF REPORT

Biallelic Variants in *SLC27A3* Cause a Complex Form of Neurodegeneration with Brain Iron Accumulation

Lorena Travaglini,¹ Cherim Jeon,² Teresa Rizza,¹ Antonio Novelli,^{1,3} Nicola Specchio,⁴ Anna Piluso,¹ Enrico Bertini,⁵ Arcangela Iuso,^{2,6} and Giacomo Garone^{4*} 

ABSTRACT: Background: Complex lipid metabolism is one of the main biological pathways disrupted in neurodegeneration with brain iron accumulation (NBIA). *SLC27A3* gene encodes for the very long-chain acyl-CoA synthetase 3, an acyl-CoA ligase that activates long and very long-chain fatty acids.

Objective: We report on a 19-year-old patient with an NBIA pattern harboring a homozygous, nonsense *SLC27A3* variant.

Methods: *SLC27A3* variants were identified using whole exome sequencing (WES). Their impact on protein function was assessed in patient fibroblasts using Western blot analysis, aerobic metabolism analysis, and fatty acid trafficking assays.

Results: The patient presented with progressive ataxia, neuropathy, optic atrophy, cognitive deterioration, mood disorder, and brain iron accumulation. WES unraveled the homozygous c.1138C>T, p.(Arg380Ter) variant in the *SLC27A3* gene. Functional studies showed that proband's variants eliminate protein expression, severely impair mitochondrial respiration, and disrupt lipid turnover.

Conclusion: Our results suggest that *SLC27A3* biallelic nonsense variant may represent a novel cause of NBIA. © 2025 The Author(s). *Movement Disorders* published by Wiley Periodicals LLC on behalf of International Parkinson and Movement Disorder Society.

Key Words: *SLC27A3*; ataxia; neuropathy; neurodegeneration with brain iron accumulation (NBIA); iron

Neurodegeneration with brain iron accumulation (NBIA) constitutes a broad range of inherited conditions whose hallmark is the accumulation of iron in the basal ganglia.¹ The clinical features consist of variable combinations of movement disorders (dystonia, parkinsonism, ataxia, and/or spasticity), epilepsy, neuropathy, cognitive deterioration, and psychiatric disorders.²

To date, 11 genes have been associated with different forms of NBIA,³ and an NBIA-like pattern can be observed in several other conditions.² The NBIA pattern can result from the disruption of different cellular pathways leading to iron dyshomeostasis, and impairment of complex lipid metabolism is the primary mechanism responsible for several NBIA's,

¹Laboratory of Medical Genetics, Translational Cytogenomics Research Unit, Bambino Gesù Children's Hospital, IRCCS, Rome, Italy; ²Institute of Neurogenetics, Helmholtz Zentrum München, Munich, Germany; ³UniCamillus—Saint Camillus International University of Health Sciences, Rome, Italy; ⁴Neurology, Epilepsy and Movement Disorders Unit, Bambino Gesù Children's Hospital, IRCCS, Rome, Italy; ⁵Research Unit of Neuromuscular and Neurodegenerative Disease, Bambino Gesù Children's Research Hospital, IRCCS, Rome, Italy; ⁶Institute of Human Genetics, School of Medicine and Health, Technical University of Munich, Munich, Germany

This is an open access article under the terms of the [Creative Commons Attribution-NonCommercial-NoDerivs](#) License, which permits use and distribution in any medium, provided the original work is properly cited, the use is non-commercial and no modifications or adaptations are made.

*Correspondence to: Dr. Giacomo Garone, Neurology, Epilepsy and Movement Disorders Unit, Bambino Gesù Children's Hospital, IRCCS, Piazza S. Onofrio, 4-00165 Rome, Italy; E-mail: giacomo.garone@opbg.net

Lorena Travaglini and Cherim Jeon have contributed equally as first authors.

Arcangela Iuso and Giacomo Garone have contributed equally as senior authors.

Relevant conflicts of interest/financial disclosures: The authors declare that there are no conflicts of interest relevant to this work. This work has been partially supported by grants of the Italian Ministry of Health ("Current Research funds"), of the European Reference Network on Rare Neurological Disease ERN-RND (project ID 739510); by #NEXTGENERATIONEU (NGEU) and the Ministry of University and Research (MIUR), National Recovery and Resilience Plan (NRRP), project MNESYS (PE0000006—a multiscale integrated approach to the study of the nervous system in health and disease (DN. 1553 11.10.2022).

Received: 5 June 2025; **Revised:** 17 September 2025; **Accepted:** 19 September 2025

Published online in Wiley Online Library (wileyonlinelibrary.com). DOI: 10.1002/mds.70079

including *PLA2G6*-, *FA2H*-, and *C19orf12*-related NBIA.

SLC27A3 gene (OMIM 604193) encodes for the very long-chain acyl-CoA synthetase 3 (ACSVL3), an acyl-CoA ligase that catalyzes the formation of fatty acyl-CoA using long (LCFA) and very long-chain fatty acids (VLCFA) as substrates.⁴

Here, we report on a 19-year-old girl with progressive ataxia, neuropathy, optic atrophy, cognitive deterioration, mood disorder, and a magnetic resonance imaging (MRI) pattern of NBIA, who was found to harbor a homozygous, nonsense *SLC27A3* variant. Using a combination of Western blot analysis, β oxidation assay, and lipid trafficking analysis in cultured fibroblasts, we showed that proband's variants eliminate protein expression, severely impair mitochondrial respiration, and disrupt lipid turnover, supporting the role of ACSVL3 deficiency as the cause of a predominantly ataxic NBIA.

Case Presentation

The proband is a 19-year-old girl of Italian ancestry, only daughter of consanguineous parents. Pregnancy and delivery were uneventful. She started walking at 18 months, and soon after gait unsteadiness and slight upper-limb tremor were observed. Language development was described as normal. At the age of 8 years, gradually emerging school difficulties were reported, and a neuropsychological evaluation demonstrated an intelligent quotient (IQ) of 61 (WISC-IV [Wechsler Intelligence Scale for Children-Fourth Edition]), leading to a diagnosis of mild intellectual disability. From age 12, a gradual worsening of gait unsteadiness, upper-limb tremor, and speech occurred. Referred to our unit at age 13, she presented gait ataxia, intention tremor, nystagmus, reduced tendon reflexes, and bilateral pes cavus. Additionally, short stature (height *z* score -2.56) was evident. A brain MRI showed bilateral T2- and SWI hypointensity of the globi pallidi, substantia nigra, and red nuclei, associated with midbrain, medulla, and cerebellar atrophy (Fig. 1). Nerve conduction studies demonstrated a sensory-motor demyelinating polyneuropathy, whereas fundoscopy, electroretinogram, and visual evoked potentials were insignificant at that time. An extensive workup for neurometabolic disorders was inconclusive (see Supporting Information).

Neuropathic pain was treated from pregabalin treatment, complex B vitamins, and acetyl L-carnitine supplementation. From age 14, the patient gradually developed obsessive thoughts, depressed mood, and disabling anxiety, requiring treatment with sertraline (75 mg/day) and aripiprazole (10 mg/day). Follow-up MRI at age 17 showed a progressive cortical atrophy, and neuropsychological evaluations demonstrated a significant IQ drop at age 18 (Wechsler Adult intelligence

Scale (WAIS) IQ 43). At last follow-up (age 19), mild bradykinesia and hypomimia were evident. In addition, reduced visual acuity (7 of 10 bilaterally) with papillary excavation and diffuse retinal pigment epithelium dystrophy on fundoscopy was observed.

Genetic Analysis

A next generation sequencing custom panel for movement disorders genes (including all known NBIA genes)⁵ was first performed and failed to identify any pathogenic variant. Whole exome sequencing (WES) was then performed in the proband and her mother (the father was unavailable for testing) on DNA extracted from peripheral blood, using the KAPA HyperExome Probes V2 Kit (Roche Diagnostics, Basel, Switzerland) for exome region enrichment and Illumina NovaSeq6000 platform for sequencing analysis. WES unraveled a homozygous, nonsense variant (GenBank: NM_024330.4, c.1138C>T, p.(Arg380Ter)) in the *SLC27A3* gene, as the strongest candidate variant (WES data were processed using an in-house implemented pipeline, and filtering strategy is summarized in Supporting Information). This variant has an allele frequency of 0.00031 in gnomAD Exome database; however, it has never been reported in homozygous state, and it is predicted to be damaging by multiple bioinformatics tools and can be classified as probably pathogenic according to ACMG criteria (PS3, PP3, PM2).⁶

Functional Studies

Western Blotting

To investigate the effects of the identified mutations on *SLC27A3* protein stability, we performed immunoblotting on fibroblast extracts from the affected individual (172096), her mother (172097), and an unrelated healthy individual (NDHF) (Fig. 2A). Under denaturing conditions, the polyclonal *SLC27A3* antibody—directed against an unspecified protein fragment—detected a main band at ~ 79 kDa in both the control and the carrier, corresponding to the canonical isoform. This band was absent in the affected individual. A second, lower-molecular-weight band was present in all samples, likely representing nonspecific antibody binding. Normalization of the *SLC27A3* signal to the loading control β -actin revealed a significant reduction in *SLC27A3* levels not only in the affected individual but also in the carrier fibroblasts (Fig. 2A).

Oxygen Consumption Rate Assay (Seahorse Metabolic Analysis)

Fibroblasts from the affected individual (172096), her mother (172097), and an unrelated healthy

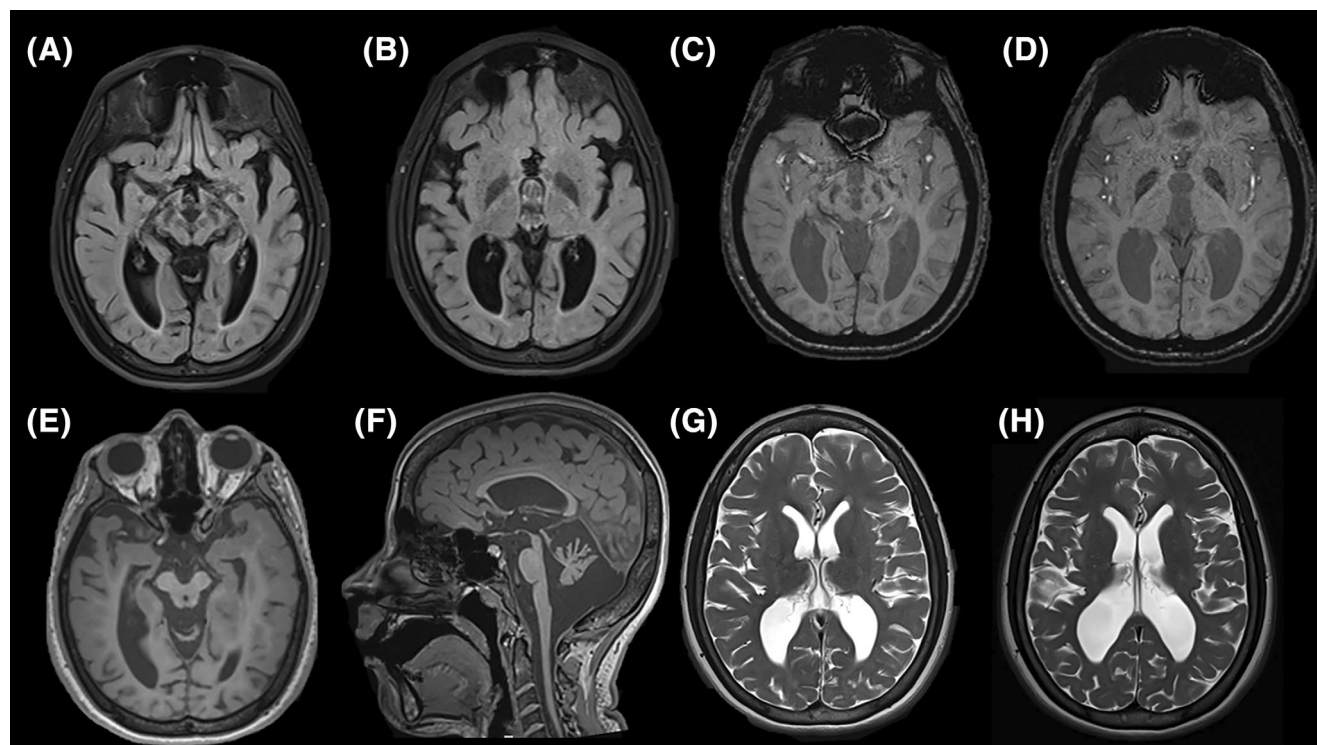


FIG. 1. Brain MRI (magnetic resonance imaging) showing red nuclei, substantia nigra, and globi pallidi hypointensity on (A, B) T2-weighted and (C, D) susceptibility-weighted images, medulla, midbrain, and cerebellar atrophy on (E, F) T1-weighted images and progressive cortical atrophy with gradual enlargement of the perisylvian subarachnoid spaces and lateral ventricles in serial MRI scans (G: 13 years, H: 18 years, T2-weighted images).

individual (NDHF) were assessed for mitochondrial respiratory capacity using pyruvate and palmitate as carbon sources. The analysis revealed reduced basal and maximal respiration with both substrates in the patient's cells compared to both the carrier and control cell lines (Fig. 2C–F). Particularly, the carrier cell line also exhibited reduced respiration compared to the healthy control. These findings suggest that the SLC27A3 mutation leads to a general mitochondrial respiration deficit, evident even in the heterozygous state and exacerbated in the homozygous state.

Fatty Acid Trafficking

To investigate potential defects in fatty acid trafficking in patient fibroblasts, cells were pulsed overnight with the fluorescent medium-chain fatty acid lauric acid (Red C12), and intracellular colocalization with mitochondria and lipid droplets (LD) was assessed after a 1-hour chase in fresh culture medium. Although no differences were observed in the short-term colocalization of fatty acids with mitochondria or LDs between the control and patient cells, staining for total LD content revealed that the patient cells accumulated more neutral lipids than controls (Fig. 2F; Supporting Information). This suggests a broader defect in fatty acid handling, potentially affecting long-term trafficking or storage.

Iron Content

To investigate potential iron accumulation in fibroblasts, cells were stained with Pearl's iron-specific reaction (blue) and counterstained with Safranin O. Fibroblasts from a Friedreich's ataxia patient and a mouse spleen tissue sample were used as positive controls (Fig. S3, Supporting Information). Patient fibroblasts exhibited no detectable iron accumulation, similar to control fibroblasts.

Discussion

NBIA includes a heterogeneous group of rare and progressive inherited conditions. Despite advances in molecular genetics, a significant proportion of individuals with a clinico-radiographic pattern of NBIA do not have variants in known NBIA or NBIA-like genes,³ suggesting that other genetic causes are yet to be identified.

Molecular pathways primarily disrupted in NBIA are heterogeneous, reflecting as iron accumulation is the final endpoint of different converging neurodegenerative processes. Except from neuroferritinopathy and aceruloplasminemia—which constitute primary disorders of iron metabolism—most NBIA genes are involved in different cellular pathways, mainly affecting coenzyme A biosynthesis (PANK2- and COASY,

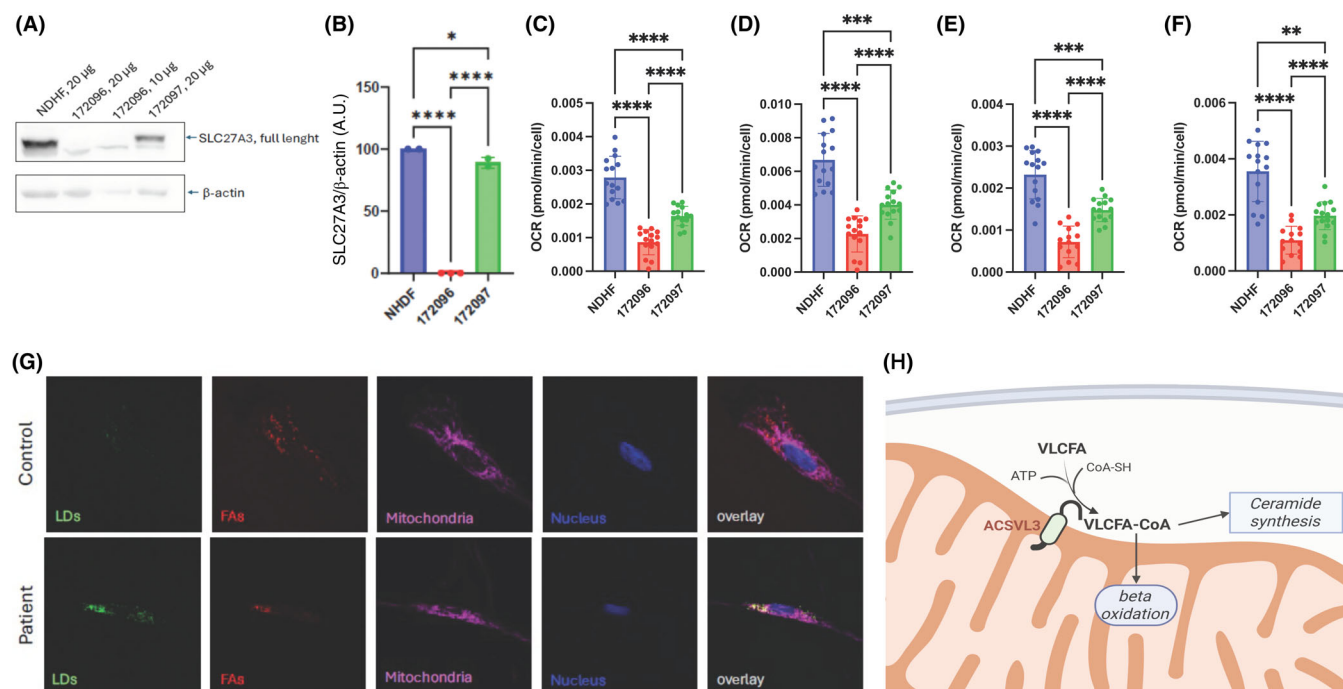


FIG. 2. Functional investigations. **(A, B)** Immunoblotting assay on fibroblast extracts shows the detection of a 79-kDa protein (corresponding to the canonical isoform) in both an unrelated healthy individual (NDHF) and the carrier mother (172097) and absent antibody binding in the patient (172096); SLC27A3/ β -actin ratio (B) confirms virtually absent protein levels in the patient and a significant reduction in protein levels also in the carrier mother compared to the control subject. Data are shown as mean \pm SD (standard deviation) of $n = 2$ (NDHF, 172097) or $n = 3$ (172096) measurements. $^*P < 0.05$ and $^{****}P < 0.0001$ (one-way ANOVA). **(C–F)** Oxygen consumption rate (OCR) assessed through Seahorse metabolic assay using pyruvate (C, D) and palmitate (E, F) as carbon source. Both basal (C and E) and maximal (D and F) assays revealed reduced respiration with both substrates in the patient's cells compared to both the carrier and control cell lines, with the carrier cell line also showing reduced respiration compared to the healthy control. Data are shown as mean \pm SD of $n = 15$ measurements. $^*P < 0.05$, $^{**}P < 0.01$, $^{***}P < 0.001$, and $^{****}P < 0.0001$ (one-way ANOVA [analysis of variance]). **(G)** Fatty acid (FA) trafficking assay. Patient cells (bottom) show lipid droplet (LD) accumulation compared to control cells (top), whereas no difference is observed in colocalization of FAs within the mitochondria or the nucleus (see Supporting Information for the fluorescence intensity plots). **(H)** Canonical function of ACSVL3 protein, catalyzing the formation of fatty acyl-CoA using long and very long-chain fatty acids as substrates. [Color figure can be viewed at wileyonlinelibrary.com]

autophagy (*WDR45*- and *ATP13A2*), and complex lipid metabolism (*PLA2G6*-, *FA2H*-, and *C19orf12*).²

In our patient, the combination of early-onset, slowly progressive ataxia, polyneuropathy, and iron deposition in the basal ganglia was clinically reminiscent of *PLA2G6*-related atypical neuroaxonal dystrophy (aNAD), suggesting a possible pathophysiological overlap between the proband's condition and aNAD. Nevertheless, the absence of seizures and the demyelinating rather than axonal pattern of nerve injury differentiated our patient's phenotype from aNAD. Therefore, it was not unreasonable to assume that a defect in lipid metabolism was the main reason to explain the proband's image.

ACSVL3 mainly functions as an acyl-CoA ligase activating LCFA and VLCFA, and is widely expressed in the brain, particularly in the cerebellum.⁴ Measurement of oxygen consumption rates in fibroblasts showed that ACSVL3 deficiency causes a severe mitochondrial respiration deficit, drastically impairing energetic metabolism. In addition, ACSVL3 deficiency led to a significant accumulation of LDs in patient's fibroblasts, suggesting a widespread disruption of intracellular lipid turnover. ACSVL3 overexpression has been found in lung cancer cell lines,

where ACSVL3 downregulation by RNA interference reduced growth rates, suggesting that ACSVL3 also regulates cellular turnover.⁴ Although the mechanisms of ACSVL3 influence on cell growth are largely unknown, it is tempting to speculate that ACSVL3 deficiency may lead to reduced neuronal proliferation during brain development and/or premature neuronal death.

Particularly, patient's fibroblasts did not exhibit overt iron accumulation, unlike other NBIA forms.^{7,8} Although more subtle impairments of iron homeostasis could be unraveled by in-depth investigations of cellular iron metabolism, this preliminary finding suggests that iron dysregulation is not a primary consequence of ACSVL3 deficiency, whereas iron accumulation could represent an epiphenomenon of impaired mitochondrial metabolism predominantly occurring in brain regions that naturally accumulate iron.

Although our findings should be replicated in further patients with similar clinical and molecular features and the role of ACSVL3 in lipid metabolism should be better elucidated in the disease-relevant neuronal cells, our results suggest that *SLC27A3* biallelic nonsense variant may represent a novel cause of NBIA. ■

Author Roles: (1) Research Project: A. Conception, B. Organization, C. Execution; (2) Statistical Analysis: A. Design, B. Execution, C. Review and Critique; (3) Manuscript Preparation: A. Writing of the First Draft, B. Review and Critique.

L.T.: 1A, 1B, 1C, 3A, 3B.
C.J.: 1A, 1B, 1C, 2A, 2B, 3A.
T.R.: 1A, 1B, 1C, 3A.
A.P.: 1A, 1B, 1C, 3A.
A.N.: 1A, 1B, 3C.
E.B.: 1A, 1B, 3C.
N.S.: 1A, 1B, 3C.
A.L.: 1A, 1B, 1C, 2C, 3A, 3B.
G.G.: 1A, 1B, 1C, 3A, 3B.

Acknowledgments: We thank the patient and her family for their support and contribution. Open access funding provided by BIBLIOSAN.

Full financial disclosures of all authors for the previous 12 months: N.S. has served on scientific advisory boards for GW Pharma (now Jazz Pharmaceuticals), BioMarin, Arvelle, Marinus, and Takeda; has received speaker honoraria from Eisai, Biogen, LivaNova, and Sanofi; and has served as an investigator for Zogenix (now a part of UCB), Marinus, Biogen, UCB, and Roche. E.B. has received honoraria for lecture presentations for Biogen and is on the advisory board for Roche, Biogen, Union Chimique Belge, and PTC Therapeutics. All other authors have no conflicts of interest that are directly relevant to the content of this article.

Data Availability Statement

The data that support the findings of this study are available on request from the corresponding author. The data are not publicly available due to privacy or ethical restrictions.

References

1. Lee J-H, Yun JY, Gregory A, Hogarth P, Hayflick SJ. Brain MRI pattern recognition in neurodegeneration with brain iron accumulation. *Front Neurol* 2020;11:1024.

2. Lehericy S, Roze E, Goizet C, Mochel F. MRI of neurodegeneration with brain iron accumulation. *Curr Opin Neurol* 2020;33(4):462–473.
3. Gregory A, Kurian AM, Wilson J, Hayflick S. Neurodegeneration with brain iron accumulation disorders overview. In: Adam MP, Feldman J, Mirzaa GM, et al., eds. *GeneReviews*®. Seattle (WA): University of Washington, Seattle; 1993[cited 2025 Apr 2]. Available from: <http://www.ncbi.nlm.nih.gov/books/NBK121988/>.
4. Pei Z, Fraisl P, Shi X, Gabrielson E, Forss-Petter S, Berger J, Watkins PA. Very long-chain acyl-CoA synthetase 3: overexpression and growth dependence in lung cancer. *PLoS One* 2013;8(7):e69392.
5. Graziola F, Garone G, Stregapede F, et al. Diagnostic yield of a targeted next-generation sequencing gene panel for pediatric-onset movement disorders: a 3-year cohort study. *Front Genet* 2019;10:1026.
6. Richards S, Aziz N, Bale S, et al. Standards and guidelines for the interpretation of sequence variants: a joint consensus recommendation of the American College of Medical Genetics and Genomics and the Association for Molecular Pathology. *Genet Med* 2015;17(5):405–424.
7. Cozzi A, Santambrogio P, Moro AS, et al. Fibroblasts and hiPS-derived astrocytes from CoPAN patients showed different levels of iron overload correlated with senescent phenotype. *Glia* 2025;73(7):1467–1482.
8. Suárez-Carrillo A, Álvarez-Córdoba M, Romero-González A, et al. Antioxidants prevent iron accumulation and lipid peroxidation, but do not correct autophagy dysfunction or mitochondrial bioenergetics in cellular models of BPAN. *Int J Mol Sci* 2023;24(19):14576.

Supporting Data

Additional Supporting Information may be found in the online version of this article at the publisher's web-site.